
Tight-binding modeling of charge migration in DNA devices

G. Cuniberti¹, E. Maciá², A. Rodriguez³, and R.A. Römer⁴

¹ Institute for Theoretical Physics, University of Regensburg, D-93040 Regensburg, Germany g.cuniberti@physik.uni-r.de

² Departamento de Física de Materiales, Universidad Complutense de Madrid, E-28040 Madrid, Spain emaciaba@fis.ucm.es

³ Dpto. Matemática Aplicada y Estadística, EUIT. Aeronáutica U.P.M., PZA Cardenal Cisneros s/n, Madrid 28040, Spain antonio.rodriuezm@upm.es

⁴ Department of Physics and Centre for Scientific Computing, University of Warwick, Coventry CV4 7AL, United Kingdom Rudolf.Roemer@warwick.ac.uk

1	Introduction and motivation	2
2	The electronic structure of DNA	3
3	Numerical techniques for charge transport in the quantum regime	4
3.1	Recursive Green function technique	5
3.2	Transfer and transmission matrix approach	6
3.3	Attaching leads	6
4	Tight-binding model approaches	8
4.1	Importance of the DNA sequence: one-dimensional models	8
4.2	Importance of base-pairing: two-channel models	11
4.3	Backbone effects: The fishbone model	13
4.4	Backbone in a ladder	15
5	Conclusions	17
	References	18

Summary. Long range charge transfer experiments in DNA oligomers and the subsequently measured — and very diverse — transport response of DNA wires in solid state experiments exemplifies the need for a thorough theoretical understanding of charge migration in DNA-based natural and artificial materials. Here we present a review of tight-binding models for DNA conduction which have the intrinsic merit of containing more structural information than plain rate-equation models while still retaining sufficient detail of the electronic properties. This allows for simulations

of transport properties to be more manageable with respect to density functional theory methods or correlated first principle algorithms.

1 Introduction and motivation

Within the class of biopolymers, DNA is expected to play an outstanding role in molecular electronics [1]. This is mainly due to its unique self-assembling and self-recognition properties which are essential for its performance as carrier of the genetic code. It is the long-standing hope of many scientists that these properties might be further exploited in the design of electronic circuits [2–6]. In the last decade of the 20th century, *transfer* experiments in natural DNA in solution showed unexpected high charge transfer rates [3, 7–10]. This suggested that DNA might support charge transport. In contradistinction, *electrical transport* experiments carried out on single DNA molecules displayed a variety of possible behaviors: insulating [11, 12], semiconducting [13, 14] and ohmic-like [15–18]. This variation might be traced to the high sensitivity of charge propagation in DNA to extrinsic (interaction with hard substrates, metal-molecule contacts, aqueous environment) as well as intrinsic (dynamical structure fluctuations, base-pair sequence) influences. Recently, experiments on single poly(GC) oligomers in aqueous solution [17] as well as on single suspended DNA with a more complex base sequence [14] have shown unexpectedly high currents of the order of 100–200 nA. Again these results, if further confirmed, suggest that DNA molecules may support rather high electrical currents given the right environmental condition.

The theoretical interpretation of these recent experiments and, in a more general context, the elucidation of possible mechanisms for charge transport in DNA have not, however, been unequivocally successful so far. While *ab initio* calculations [19–28] can give at least in principle a detailed account of the electronic and structural properties of DNA, the huge complexity of the molecule and the diversity of interactions present preclude a complete treatment for realistic molecule lengths. When interactions with counter ions and hydration shells or vibrational degrees of freedom are to be considered, the situation easily becomes untractable. On the other hand, model-based Hamiltonian approaches to DNA [29–44] have been already been discussed in great detail and can play a complementary role by addressing single factors that influence charge transport in DNA. However, here it is of course clear neither a-priori nor a-posteriori (given the aforementioned experimental situation) which model should be used. Somewhat mirroring the experimental situation, a large variety of models exist and the results are not necessarily consistent across different models.

In this contribution, we review tight-binding models of DNA which have been proposed in the literature and argued to reproduce experimental [29] as well as *ab-initio* results [45]. We first concentrate on simple one- and two-channel models of DNA in which the main transport mechanism is concen-

trated in the effects of π -overlap in the base or base-pair sequences. The models are usually constructed to take into account the HOMO-LUMO gap of the single base pairs similar to many of the DFT-based studies. A main feature of the next class of models is the presence of sites which represent the sugar-phosphate backbone of DNA but along which no electron transport is permissible. These models construct a gap due to transversal perturbation of the π -stack, i.e. even when the onsite energies are constant. The aim of this review is thus to explain the present state of affairs in the tight-binding-model-based approach and we will be very brief on many others aspects of the charge migration problem, as these are already well treated in the other chapters of this book.

2 The electronic structure of DNA

DNA is a macro-molecule consisting of repeated stacks of bases formed by either AT (TA) or GC (CG) pairs coupled via hydrogen bonds and held in the double-helix structure by a sugar-phosphate backbone. In Fig. 1, we show a schematic drawing. The electronic energetics of a double-stranded DNA chain should take into account three different contributions coming from (i) the nucleobase system, (ii) the backbone system and (iii) the environment, as it is sketched in Fig. 2. Attending to the energies involved in the different interactions, the resulting energy network can be hierarchically arranged, starting from high energy values related to the on-site energies of the bases and sugar-phosphate groups (8 – 12 eV) [46,47] passing through intermediate energy values related to the hydrogen bonding between Watson-Crick pairs (~ 0.5 eV) [46] and the coupling between the bases and the sugar moiety (~ 1 eV) [47] and ending up with the aromatic base stacking low energies (0.01 – 0.4 eV) [46,48]. The energy scale of environmental effects (1 – 5 eV) is related to the presence of counter ions and water molecules, interacting with the nucleobases and the backbone by means of hydration, solvation and charge transfer processes. It is about one order of magnitude larger than the coupling between the complementary bases, and about two orders of magnitude larger than the base stacking energies.

We emphasize that in many of the models to be reviewed later in this chapter, simplified assumptions about these energy scales are employed. Mostly, however, the ionization energies $\epsilon_G = 7.75$ eV, $\epsilon_C = 8.87$ eV, $\epsilon_A = 8.24$ eV and $\epsilon_T = 9.14$ eV, [48–52] are taken as suitable approximations to the onsite energetics at each base.

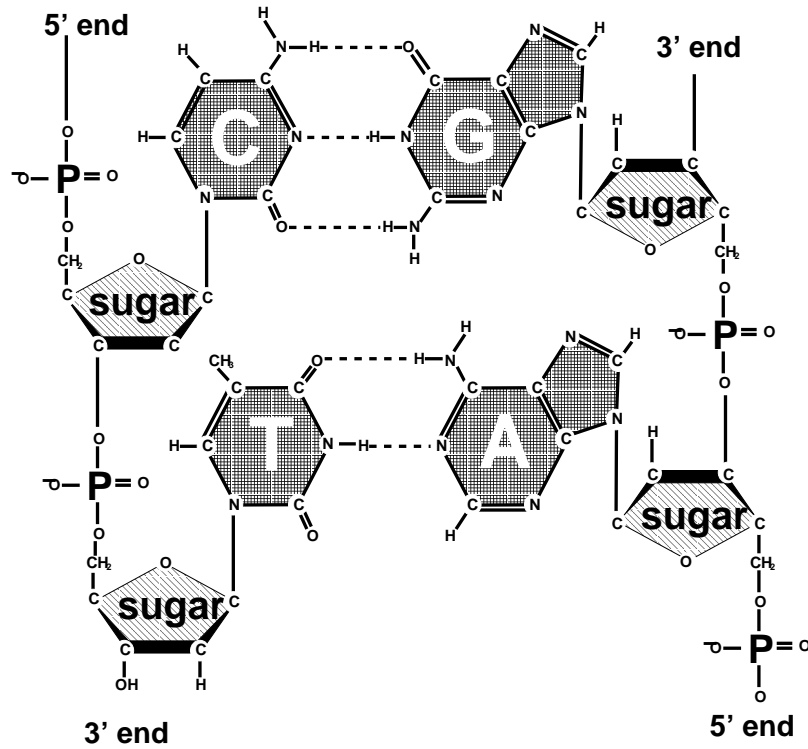


Fig. 1. The chemical composition of DNA with the four bases Adenine (A), Thymine (T), Cytosine (C), Guanine (G) and the backbone. The backbone is made of phosphorylated sugars shown in light grey, the nucleobases are indicated in dark grey.

3 Numerical techniques for charge transport in the quantum regime

Before we in the following turn our attention to the variety of simplified models which have been proposed to capture the essential charge transport features of DNA, let us briefly recall some of the techniques used to investigate these.

There are several approaches suitable for studying the transport properties of quasi-one-dimensional tight-binding models for long DNA and these can be found in the literature on transport in solid state systems, or, perhaps more appropriately, quantum wires [53]. Since the variation in the sequence of base pairs precludes a general solution, one normally uses methods well-known from the theory of disordered systems [54, 55]. The main advantage of these methods is that they work reliably (i) for the relatively short DNA strands ranging from 13 base pairs (as in DFT studies [56]) up to 30 base pairs length which are being used in the nanoscopic transport measurements [13] as well as (ii) for somewhat longer DNA sequences as modeled in the

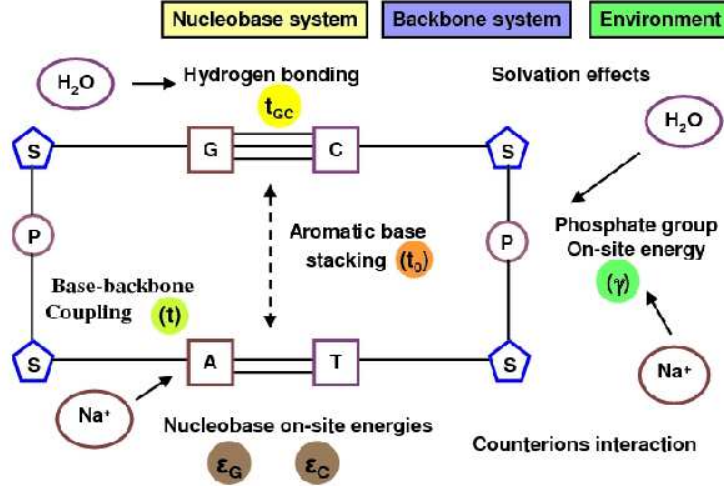


Fig. 2. Sketch illustrating the overall energetics of a double-stranded DNA chain.

electron transfer results and (iii) even for complete DNA sequences which contain, e.g. for human chromosomes up to 245 million base pairs [57]. We measure the effectiveness of the electronic transport by various measures such as the *localisation length* ξ , participation numbers, etc. These roughly speaking parameterise whether an electron is confined to a certain region of the DNA (resulting in insulating behavior) or can proceed across the full length L of the DNA molecule (metallic behavior).

3.1 Recursive Green function technique

The first method one can use is the recursive Green function approach pioneered by MacKinnon [58, 59]. It can be used to calculate the dc and ac conductivity tensors and the density of states (DOS) of a d -dimensional disordered system and has been adopted to calculate all kinetic linear-transport coefficients such as thermoelectric power, thermal conductivity, Peltier coefficient and Lorenz number [60, 61]. Briefly, the approach utilizes the advanced and retarded Green's functions, $\mathcal{G}^-(E - i0^+)$ and $\mathcal{G}^+(E + i0^+)$, respectively, and the usual definition $[(E \pm i0^+)\delta_{ij} - H_{ij}]G_{ij}^\pm = \delta_{ij}$, where G_{ij}^\pm is the matrix element $\langle i|\mathcal{G}^\pm|j\rangle$ and H_{ij} is similarly the matrix element of the Hamiltonian [61]. δ_{ij} denotes the Kronecker δ between basis states $\{|i\rangle\}$. If contains only nearest-neighbor connections, then these expressions can be written interactively as

$$-H_{ii+1}G_{i+1j}^\pm = \delta_{ij} - [(E \pm i0)\delta_{ij} - H_{ij}]G_{ij}^\pm + H_{ii-1}G_{i-1j}^\pm. \quad (1)$$

Here $H_{ii\pm 1}$ are the terms in the Hamiltonian connecting slice i with its neighboring slices $i \pm 1$. If we now reinterpret the left index i as a pseudo time, then we see that the future Green function slice $i + 1$ can be constructed by the present slice at i and the previous slice at $i - 1$. The method is well suited to study coherent transport properties and can be extended to include incoherent processes as well [62].

3.2 Transfer and transmission matrix approach

The next method of choice is the iterative transfer-matrix method (TMM) [54, 63–66] which allows us in principle to determine the localisation length ξ of electronic states in systems with varying cross section M and length $L > M$. This localization length describes the decay of the wave function for transport along a quasi one-dimensional system and ξ may be used as a rough guide of the extend of electronic states.

For disordered systems, typically a few million sites $L \gg M$ are needed to achieve reasonable accuracy for ξ [54]. However, in the present situation we are interested in finding ξ also for DNA strands of typically only a few hundred or a few ten thousand base-pair long sequences. Thus in order to restore the required precision, one modifies the conventional TMM and now performs the TMM on a system of fixed length L_0 . This modification has been previously used [67–69] and may be summarized as follows: After the usual forward calculation with a global transfer matrix \mathcal{T}_{L_0} , we add a backward calculation with transfer matrix $\mathcal{T}_{L_0}^b$. This forward-backward-multiplication procedure is repeated K times. The effective total number of TMM multiplications is $L = 2KL_0$ and the global transfer-matrix is $\tau_L = (\mathcal{T}_{L_0}^b \mathcal{T}_{L_0})^K$. It can be diagonals as for the standard TMM with $K \rightarrow \infty$ to give $\tau_L^\dagger \tau_L \rightarrow \exp[\text{diag}(4KL_0/\xi_i)]$. The largest ξ_i for all $i = 1, \dots, M$ then corresponds to the localisation lengths of the electron on the DNA strand and will be measured in units of the DNA base-pair spacing (0.34 nm). Let us emphasize that the above approach converges even for $L < \xi$. However, in that case, values of ξ clearly are dominated by finite-size and boundary effects and their significance is no longer quantitative, but qualitatively indicates extended states smeared out over the finite system length L . Last, the transmission coefficient $T_L(E)$, related to the Landauer conductance g via $g = (2e^2/h)T_L(E)/(1 - T_L(E))$ [70–72], is defined in terms of the matrix elements of τ_L .

3.3 Attaching leads

Let us assume that, as a first approximation, we can consider a DNA model in terms of a linear chain with an orbital per site, where each lattice site

represents a base pair. The ends of the chain are connected to leads modeled as semi-infinite one-dimensional chains of atoms with one orbital per site. Broadly speaking, one expects the binding to metallic leads would affect the electronic structure of the molecule. If so, we should consider the states belonging to the coupled molecular-metallic system rather than those of the molecular subsystem alone [73]. Thus we shall consider henceforth that the coupling between the contacts and the molecule is weak enough, so that the lead-molecule-lead junction can be properly described in terms of three non-interacting subsystems [74, 75], according to

$$\begin{aligned}
 H = & H_{\text{DNA}} - t_{\text{Contact}} (|0\rangle\langle 1| + |N\rangle\langle N+1| + h.c.) \\
 & + \sum_{k=0}^{-\infty} \varepsilon_{\text{Lead}} |k\rangle\langle k| - t_{\text{Lead}} |k-1\rangle\langle k| + h.c. \\
 & + \sum_{k=N+1}^{+\infty} \varepsilon_{\text{Lead}} |l\rangle\langle l| - t_{\text{Lead}} |l\rangle\langle l+1| + h.c.. \quad (2)
 \end{aligned}$$

In Eq.(2), H_{DNA} is the DNA Hamiltonian, the second term describes the DNA-lead contact, and the last two terms describe the contacts at both sides of the DNA chain, where N is the number of base pairs, ε_n are the on-site energies of the base pairs, t_{Contact} is the hopping strength between the leads and the end nucleotides, $\varepsilon_{\text{Lead}}$ is the leads on-site energy and t_{Lead} is their hopping term.

The Green function methods are well-suited to include contact effects since their boundary conditions at the contacts require specification of a suitable Green function in the leads which can be chosen to model the geometry of contacts. The TMM usually starts assuming a particle-like injection of carriers into the transport channels and a proper treatments of leads is lacking, but the extracted localization lengths at least for long chains are largely independent of the exact choice. Irrespective of numerical methods used, most earlier tight-binding studies assumed perfect coupling to metallic leads or simply ignore the issue altogether. The role of contact effects within the TMM framework was recently reported for a poly(GACT) tetra-nucleotide in Ref. [76] in terms of two contact matrices which explicitly take into account the presence of the t_{Contact} hopping integral. Depending on the value adopted for t_{Contact} , the obtained transmission coefficient does not reach in general the full transmission condition $T_L(E) = 1$ due to the symmetry breaking related to the coupling of the G (T) end nucleotides at the left (right) leads, respectively. This extreme sensitivity is due to interference effects between the DNA energy levels and the electronic structure of the leads at the metal-DNA interface, and indicates that the *optimal* system configuration for efficient charge transfer is determined by the resonance condition $t_{\text{Contact}} = \sqrt{t \cdot t_{\text{Lead}}}$. Quite interestingly, one realizes that, due to resonance effects, a stronger coupling to the leads not always result in a larger conductance through the system, in agreement with the results obtained by Guo and co-workers for the transmission

coefficient of poly(G)-poly(C) molecules making use of the Green function technique [77]. Subsequent works have exploited the existence of this optimal charge injection condition to study the charge migration efficiency through more realistic duplex chains (see the contribution by Apalkov, Wang, and Chakraborty in this volume)

In general, modeling the geometry and bonding character of the contact at the interface is a very delicate issue, since detailed information on both the metal geometry and DNA chemical bonding at the contacts is poorly known to date. Consequently, in most modeling of the DNA-contact interface, the parameter t_{Contact} deals with the tunneling probability between the frontier orbitals, thus roughly encompassing bonding effects at the interface. Recent transport experiments have shown that deliberate *chemical bonding* between DNA and electrodes is a prerequisite for achieving reproducible conductivity results [12, 78, 79]. Accordingly, the study of contact effects on the charge migration efficiency is an important issue to be considered in realistic models of DNA transport.

4 Tight-binding model approaches

The ab initio methods are clearly very powerful. However, from a physics perspective, the question immediately arises if an even simpler, effective model approach, might capture the essentials of charge migration equally well. This strategy is known as the tight-binding approach to DNA — note that in this language the term *tight-binding* is used somewhat differently from the terminology of theoretical chemistry. This simple approach has been used right from the start of the physics involvement in DNA research. The idea is to capture the main path-ways of charge migration along the DNA molecule stack in a simple model of *sites* and *hopping strengths*. Charge transport along this model is then described by simple tight-binding orbitals on the sites and suitably parametrized hopping onto neighboring sites. The advantage is this approach should be clear: once the appropriate onsite energies and hopping strengths are known, much larger system sizes can be studied than with the ab initio methods. The downside of course is that the determination of the effective parameters and in particular the choice which to leave out completely will be at least to some degree a matter of personal preference and thus open to criticism.

4.1 Importance of the DNA sequence: one-dimensional models

The simplest TB model of the DNA stack can be constructed as a one-dimensional model as given in Fig. 3. There is a single central conduction channel in which individual sites represent a base-pair. Every link between sites implies the presence of a hopping amplitude. The Hamiltonian for this *wire* model (H_W) is given by

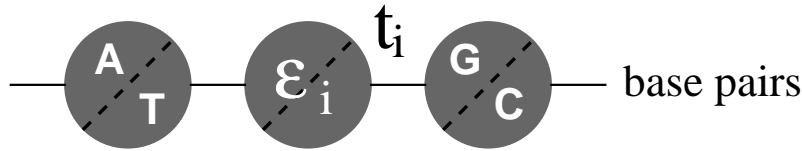


Fig. 3. The line model for electronic transport along DNA corresponding to the Hamiltonian given in Eq. (3). Lines denote hopping amplitudes and circles give the central (grey) nucleobase pairs.

$$H_W = \sum_{i=1}^L -t_i |i\rangle \langle i+1| - t_{i-1} |i\rangle \langle i-1| + \varepsilon_i |i\rangle \langle i| \quad (3)$$

where t_i is the hopping between nearest-neighbour sites $i, i+1$ along the central branch and we denote the onsite energy at each site along the central branch by ε_i . L is the number of sites/bases in the sequence. For constant $t_i = t$, $\varepsilon_i = 0$ and open boundary conditions, the spectrum of the model is given by

$$E = -2t \cos\left(\frac{\pi k}{L+1}\right) \quad (4)$$

with $k = 1, 2, \dots, L$. For random choice of onsite energies or hopping strengths, this model is well-known as the Anderson model [80] with diagonal or off-diagonal disorder and its transport properties are governed by one-dimensional Anderson localization [81].

In order to use this Hamiltonian to model DNA, one needs to know the appropriate parameters for onsite energies and hopping strengths [48–52], or, alternatively, argues that mostly the statistical properties of these quantities determine the transport. For natural DNA sequences, a useful choice for the onsite energies might be the ionization potentials mentioned in section 2. But since base-pairs are modelled by a single site, the DNA is effectively described as a sequence of GC (identical to CG) and AT (or TA) pairs with links between like (GC-GC or AT-AT) or unlike (GC-AT, AT-GC) pairs. Thus the model parameters for the pairs should be computed as suitable estimates based on the ionization potentials of individual bases [48–52].

Already such a simple model as (3) allows to study various aspects of charge transport in DNA. Electrical transport through individual DNA molecules was studied in Ref. [82], using poly(G)-poly(C) DNA. Individual molecules are coupled to external baths [83], thus leading to partial decoherence. Good agreement with the experimental results of Ref. [13] is demonstrated. A twist angle in the hopping parts of (3) is used in Ref. [84] to model the effect of thermal fluctuations on transport in DNA. The participation ratio is used to estimate the extent of the electronic states. Assuming that inelastic effects due to temperature can be ignored, the paper then computes the temperature dependence of the conductivity. The transmission spectrum for a chain of poly(G)-poly(C) DNA molecules was studied in Ref. [77] where

also disorder and contact effects were taken into account. The model contains various parameters according to the HOMO/LUMO structure of DNA. Furthermore, charging effects, i.e. Coulomb blockade, were studied within a mean-field approach. For a DNA chain consisting of AT and GC pairs, Ref. [85] investigates structural and dynamical disorder. Here, in addition to the on-site energies in (3), also the hopping elements t_i are chosen according to the specific DNA sequence, which itself, however, consists of random sequences of A,T,G,C nucleotides. It is shown that both types of disorder can significantly influence the transport properties. Ref. [86] studies both (quasi-)coherent and incoherent transport regimes using Landauer and Kubo formalism via a continued fraction approach for poly(G)-poly(C) and also poly(A)-poly(T) DNA chains. Superexchange-like exponential length dependence is found for the coherent and Ohmic-like behavior for the incoherent regimes.

The next group of studies focuses on the influence that possible correlations in both artificial and natural DNA sequences might have on the transport. Natural λ -phage DNA has been investigated in Ref. [33] within a transfer-matrix approach. Transmission spectra are shown to be very different from poly(G)-poly(C) DNA. The results are argued to be roughly consistent with those from electron *transfer* studies. The influence of long-range correlations in DNA sequences is studied in Ref. [32]. Natural DNA of the first completely sequenced human chromosome 22 (Ch22) is compared to artificial sequences such as random and Fibonacci sequences. It is found that long-range correlations induce coherent charge transfer over longer lengths scales, at least for Ch22. Ref. [87] uses the same numerical method as Ref. [32] and corroborates the results for Ch22 by comparing to a Rudin-Shapiro sequence. An intriguing relation between the length of a region in coding DNA versus non-coding DNA and a repeatedly higher transport characteristic in coding DNA was reported in Refs. [88,89].

The influence of temperature and associated structural fluctuations of DNA and thus the onsite and hopping parameters has been studied in the next group of papers. Ref. [90] investigates a polaronic model in which the hopping elements are influenced by vibrations along the chain. It is shown that a polaron can indeed form for reasonable values of parameters. Ref. [91] studies a similar situation, but also takes into account the rotation between base pairs along the DNA stack. The paper is actually aimed at charge transfer and proposes that the thermal fluctuations are the limiting step for site-to-site charge transfer. Polarons, which have a “twist” and can thus model the double-helix structure of DNA better, are investigated in Ref. [92]. Non-linear effects are taken into account and it is shown that these lead to different polaronic behavior. In Ref. [93], it is argued that polaronic transport can be trapped by the thermal denaturation of poly(G)-poly(C) DNA. Thermal effects are modelled by an anharmonic Morse potential. Semi-empirical quantum-chemical calculations were performed in Ref. [94] for poly(G)-poly(C) and also for poly(A)-poly(T) DNA using a polaron model. Localization lengths of charge states

larger than 2000 base pairs have been computed and it was shown that significant differences between poly(G)-poly(C) and poly(A)-poly(T) DNA exist.

Besides temperature, the solution in which DNA is prepared or measured, its geometry and bend as well as the properties of the contacts to external leads will influence the measured transport characteristics. The influence of disorder for (3) has been investigated in Ref. [85]. Contact effects were studied by Ref. [76] for poly(GACT) chains. Resonance conditions were identified which show that a strong coupling to the leads does not always result in larger conductance.

The simple wire model (3) has also been used for studies of charge transfer. Briefly, DNA bridges, containing only AT base pairs, were investigated in Ref. [95] and decay lengths comparable with single-step tunneling were found. The presence of Kondo bound states [96] leads to long tunneling lengths above 100nm. Similarly, time-dependent random hopping strenghts were studied in Ref. [97] and analyzed in a charge transfer context. Last, a soliton-based explanation for charge transfer in long segments of DNA was given in Ref. [98].

4.2 Importance of base-pairing: two-channel models

A central simplification of the wire model is the description of a DNA base-pair as a single site. By doing so, one loses the distinction between a pair with G (or A) on the 5' end of the DNA and a C (or T) on the 3' side and one where C sits on the 5' and G on the 3', i.e. GC is equal to CG. This distinction becomes important when considering hopping between base-pairs, e.g. the hopping from GC to AT is different from CG to AT because of the different size of the DNA bases and thus the different overlap between G to A and C to A (and similarly for C to T and G to T) [99]. Furthermore, the relevant electronic states of DNA (highest-occupied and lowest-unoccupied molecular orbitals with and without an additional electron) are localised on one of the bases of a pair only [100]. The reduction of the DNA base-pair architecture into a single site per pair, as in the wire model (3), is obviously a highly simplified approach.

This deficiency of the wire model may be overcome by modelling each DNA base as an independent site. The hydrogen-bonding between base-pair is then described as an additional hopping perpendicular to the DNA stack as shown in Fig. 4. There are two central branches, linked with one another, with interconnected sites where each represents a complete base. This *two-channel* model is a planar projection of the structure of the DNA with its double-helix unwound, and still without regard for the backbone. We note that results for electron transfer also suggest that the transfer proceeds preferentially down one strand [3]. The Hamiltonian now reads

$$H_L = \sum_{i=1}^L \left[\sum_{\tau=1,2} (t_{i,\tau} |i, \tau\rangle \langle i+1, \tau| + \varepsilon_{i,\tau} |i, \tau\rangle \langle i, \tau|) \right]$$

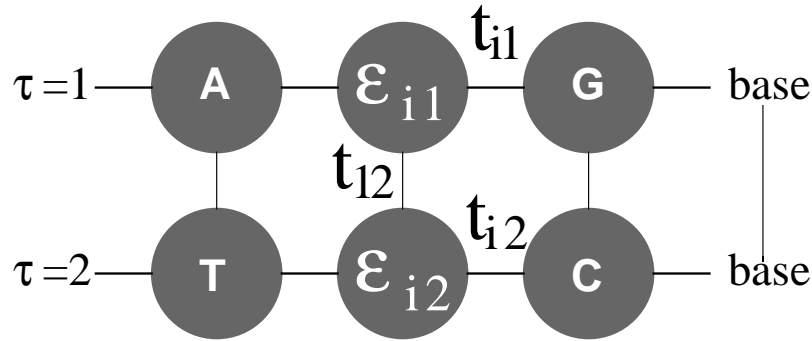


Fig. 4. The two-channel model for electronic transport along DNA. The model corresponds to the Hamiltonian (5). Electronic pathways are shown as lines, whereas the nucleobases are given as (grey) circles.

$$+ t_{1,2}|i, 1\rangle\langle i, 2| + h.c. \quad (5)$$

where $t_{i,\tau}$ is the hopping amplitude between sites along each branch $\tau = 1, 2$ and $\epsilon_{i,\tau}$ is the corresponding onsite potential energy. The new parameter t_{12} represents the hopping between the two central branches, i.e., perpendicular to the direction of conduction. As before, we may now attempt to use ab-initio methods to compute t_{12} or simply model it relative to the strength of the parallel hopping $t_{i,\tau}$. For the ordered system with $t_{i,\tau} = t$ and $\epsilon_{i,\tau} = 0$, the two channel model is just a special case of the 2D rectangular system with spectrum $-2t_x \cos\left(\frac{\pi k_x}{L_x+1}\right) - 2t_y \cos\left(\frac{\pi k_y}{L_y+1}\right)$, $k_x = 1, 2, \dots, L_x$, $k_y = 1, 2, \dots, L_y$. Thus we find

$$E = -2t \cos\left(\frac{\pi k}{L+1}\right) \mp t_{1,2} \quad (6)$$

where the minus (plus) sign corresponds to even, $\psi_{n,1} = \psi_{n,2}$, (odd, $\psi_{n,1} = -\psi_{n,2}$) states with the same (opposite) sign for the wave function on each strand. For random onsite disorder, the system is again localized and the localization lengths are known for different energies and disorder values [101].

Iguchi was one of the early authors to suggest that a two-leg ladder model might be a useful starting point [102]. A band gap like behavior was found in Ref. [103], which also considered the Coulomb repulsion between different bases. It was further shown that for engineered DNA — modelled as frustration — the band vanishes. Ref. [34] used the two-leg ladder model to study the spatial extent of electronic states in long DNA chains. They found that the extent varies considerably depending on the sequence, but remains rather small. Recently, Caetano and Schulz found very large participation ratios in the two-leg ladder at finite system sizes [104]. They speculated that this might indicate a transition to effectively delocalized states. But this claim is not expected to hold for longer chains [105–107]. The influence of electronic spin and

interactions has been studied in Ref. [36]. This work concentrates on charge transfer aspects and shows that interaction opens a gap in the electronic states of AT and GC pairs. Further transport properties of Ch22, as well as λ -phage and the histone protein, are investigated in Ref. [41] and compared to artificial DNA. It is notable that while the model used in [41] is a two-leg ladder, the rungs of the ladder are now modeling not the π transport channels but rather the charge migration along the sugar-phosphate backbone. This approach is similar to Ref. [108]. Discrete breather-type solutions caused by environmental effects were studied in a two-leg ladder already in Ref. [109]. A Morse potential was used to represent hydrogen bonding. The breathers were found to be pinned by the discrete lattice or trapped in defect regions. A similar model based on the non-linear Schrödinger equation was studied in Ref. [110], where the transport of the solitons was assumed to propagate along the sugar-phosphate backbone.

4.3 Backbone effects: The fishbone model

This *fishbone model*, shown in Fig. 5, retains the central conduction channel in which individual sites represent a base-pair. However, these are now interconnected and further linked to upper and lower sites, representing the backbone. The backbone sites themselves are *not* interconnected along the backbone. Every link between sites implies the presence of a hopping amplitude. The Hamiltonian for the fishbone model (H_F) is given by

$$H_F = \sum_{i=1}^L \sum_{q=\uparrow,\downarrow} (-t_i|i\rangle\langle i+1| - t_i^q|i, q\rangle\langle i| + \varepsilon_i|i\rangle\langle i| + \varepsilon_i^q|i, q\rangle\langle i, q|) + h.c. \quad (7)$$

where t_i is the hopping along the central branch and t_i^q with $q = \uparrow, \downarrow$ gives the hopping from each site on the central branch to the upper and lower backbone respectively. We denote the onsite energy at each site along the central branch by ε_i and, additionally, the onsite energy at the sites of the upper and lower backbone is given by ε_i^q , with $q = \uparrow, \downarrow$. L is the number of sites/bases in the sequence. It is easy to see that the existence of the backbone leads to an effectively renormalized and energy-dependent disorder

$$\left(\varepsilon_n - \frac{t^{\uparrow 2}}{\varepsilon_n^{\uparrow} - E} - \frac{t^{\downarrow 2}}{\varepsilon_n^{\downarrow} - E} \right) \quad (8)$$

at each base pair n on the π stack. If, we as before for the wire model (3), consider the ordered situation $t_i = t$, $t^{\uparrow} = t^{\downarrow}$, $\varepsilon_i = \varepsilon_i^{\sigma} = 0$ for $\sigma = \uparrow, \downarrow$, we find that the energies are now given by

$$E_{\pm} = -2 \cos\left(\frac{\pi k}{L+1}\right) \pm \sqrt{t^2 \cos^2\left(\frac{\pi k}{L+1}\right) + 2t^{\uparrow 2}} \quad (9)$$

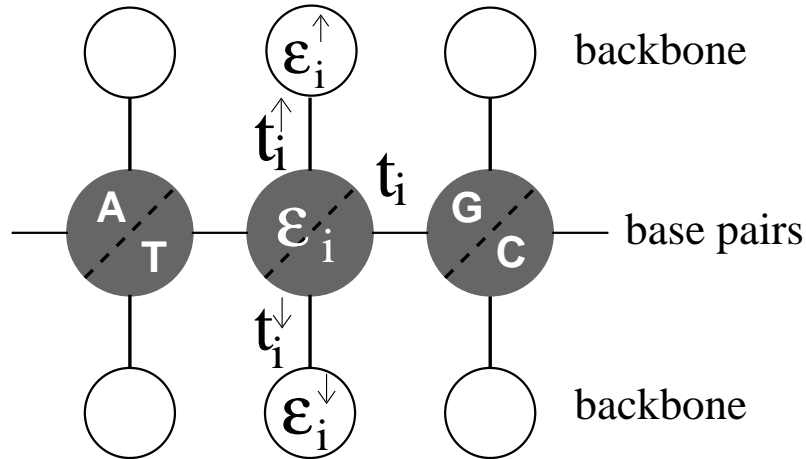


Fig. 5. The fishbone model for electronic transport along DNA corresponding to the Hamiltonian given in Eq. (7). Lines denote hopping amplitudes and circles give the central (grey) nucleobase pairs and backbone (open) sites.

for $k = 1, 2, \dots, L$. Hence, there is a highly degenerate state at $E = 0$ corresponding to all the backbone sites and the original single-band of (4) splits into two cosine bands such that

$$E \in \left[-t - \sqrt{t^2 + 2t^{\uparrow 2}}, -t + \sqrt{t^2 + 2t^{\uparrow 2}} \right] \cup \left[t - \sqrt{t^2 + 2t^{\uparrow 2}}, t + \sqrt{t^2 + 2t^{\uparrow 2}} \right]. \quad (10)$$

In Ref. [29] it had been shown that this model when applied to an artificial sequence of repeated GC base pairs, poly(G)-poly(C) DNA, reproduces experimental data current-voltage measurements when $t_i = 0.37$ eV and $t_i^q = 0.74$ eV are being used. Therefore, we will assume $t_i^q = 2t_i$ and set the energy scale by $t_i \equiv 1$ for hopping between GC pairs. Furthermore, since the energetic differences in the adiabatic electron affinities of the bases are small [111], we choose $\epsilon_i = 0$ for all i .

The physics of the fishbone model was first discussed for poly(G)-poly(C) in Ref. [29]. In fact, the central sites of the fishbone are to model the G nucleotide only, with the effect of the C bases neglected as not so relevant for transport due to their different onsite HOMO/LUMO energies. The model was then independently studied by Zhong [112] for random and natural DNA sequences and he also found an interesting transport enhancing effect in the band gap upon increasing potential disorder. A further study [40] revealed that the extent of electronic states in the two bands of the model can be up to a few dozen base pairs large. Furthermore, upon adding binary disorder, intended to model adhesion of ions from the ionic solution in which DNA strands exist, the band gap closes and the size of initially very well localized band-gap states can be made to increase substantially [113]. This effect was

also studied in Refs. [38,39] where the system was coupled to a phonon bath. Here, the band gap was shown to close with increasing temperature and the temperature dependence of the charge transmission near the Fermi energy is exponential.

4.4 Backbone in a ladder

Combining the advantages of the fishbone and the two-channel models, we now model each base as a distinct site where the base pair is then weakly coupled by the hydrogen bonds. The resulting *ladder* model is shown in Fig. 6. There are two central branches, linked with one another, with interconnected

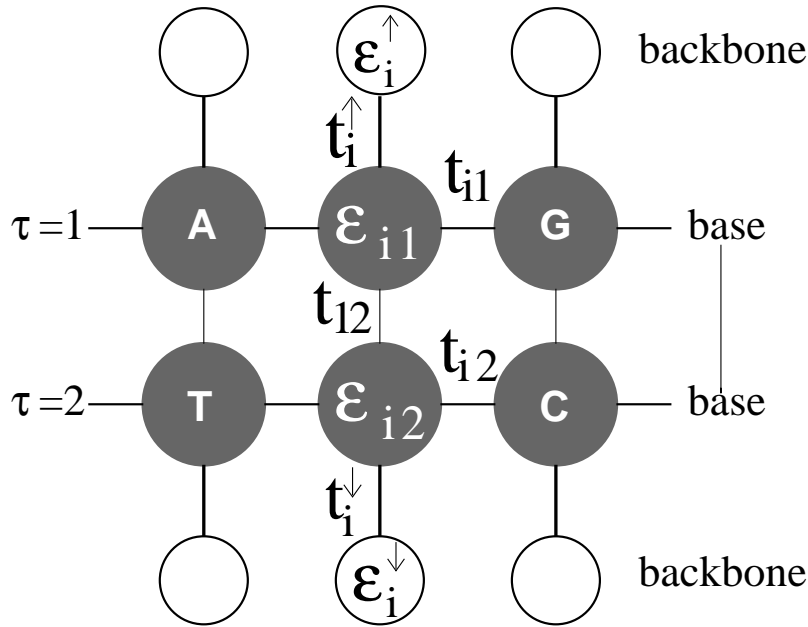


Fig. 6. The ladder model for electronic transport along DNA. The model corresponds to the Hamiltonian (5) and the reader should compare the figure to Figs.(4) and (5).

sites where each represents a complete base and which are additionally linked to the upper and lower backbone sites. The backbone sites as in the fishbone model are not interconnected. In fact, first principle calculations, showing that the phosphate molecular orbitals are systematically below the base related ones, do not favor the possible hopping of charge carriers between successive phosphate groups along the backbone. [114] The Hamiltonian for the ladder model is given by

$$\begin{aligned}
H_L = & \sum_{i=1}^L \left[\sum_{\tau=1,2} (t_{i,\tau}|i,\tau\rangle\langle i+1,\tau| + \varepsilon_{i,\tau}|i,\tau\rangle\langle i,\tau|) \right. \\
& + \sum_{q=\uparrow,\downarrow} (t_i^q|i,\tau\rangle\langle i,q(\tau)| + \varepsilon_i^q|i,q\rangle\langle i,q|) \\
& \left. + t_{1,2}|i,1\rangle\langle i,2| \right] + h.c. \tag{11}
\end{aligned}$$

where as before in (5) $t_{i,\tau}$ is the hopping amplitude between sites along each branch $\tau = 1, 2$ and $\varepsilon_{i,\tau}$ is the corresponding onsite potential energy. t_i^q and ε_i^q as in (7) give hopping amplitudes and onsite energies at the backbone sites. Also, $q(\tau) = \uparrow, \downarrow$ for $\tau = 1, 2$, respectively. The parameter t_{12} represents the hopping between the two central branches as for the two channel model (5).

For the ordered system with $t_{i,\tau} = t$, $t^\uparrow = t^\downarrow$, $\varepsilon_{i,\tau} = \varepsilon_i^\sigma = 0$, we find again that the presence of the backbone sites leads to an effective renormalization of onsite energies along the two base pair strands with energy-dependent disorder

$$\epsilon_{n,\tau} - \frac{t^{\sigma 2}}{E - \epsilon_\tau^\sigma} \tag{12}$$

and $(\tau, \sigma) = (1, \uparrow)$ or $(2, \downarrow)$. The energies for even states are

$$E^+ = \frac{1}{2} \left\{ -t_{1,2} - 2t \cos\left(\frac{\pi k^+}{L+1}\right) \pm \sqrt{\left[t_{1,2} + 2t \cos\left(\frac{\pi k^+}{L+1}\right)\right]^2 + 4t^{\uparrow 2}} \right\} \tag{13}$$

with $k^+ = 1, 2, \dots, L$. Similarly, the odd states have energies

$$E^- = \frac{1}{2} \left\{ t_{1,2} + 2t \cos\left(\frac{\pi k^-}{L+1}\right) \pm \sqrt{\left[t_{1,2} - 2t \cos\left(\frac{\pi k^-}{L+1}\right)\right]^2 + 4t^{\uparrow 2}} \right\} \tag{14}$$

and $k^- = 1, 2, \dots, L$. Thus we again have two energy bands, with a slightly smaller gap, given as

$$\begin{aligned}
E \in & \left[-\left(t + \frac{t_{1,2}}{2}\right) - \sqrt{\left(t + \frac{t_{1,2}}{2}\right)^2 + t^{\uparrow 2}}, \left(t + \frac{t_{1,2}}{2}\right) - \sqrt{\left(t + \frac{t_{1,2}}{2}\right)^2 + t^{\uparrow 2}}, \right. \\
& \left. \cup \left[-\left(t + \frac{t_{1,2}}{2}\right) + \sqrt{\left(t + \frac{t_{1,2}}{2}\right)^2 + t^{\uparrow 2}}, \left(t + \frac{t_{1,2}}{2}\right) + \sqrt{\left(t + \frac{t_{1,2}}{2}\right)^2 + t^{\uparrow 2}} \right] \right] \tag{15}
\end{aligned}$$

In Ref. [40], electronic transport in this model was measured by the *localisation length* ξ , which roughly speaking parametrises whether an electron is confined to a certain region ξ of the DNA (insulating behaviour) or can proceed

across the full length L ($\leq \xi$) of the DNA molecule (metallic behaviour). Various types of disorder, including random potentials, were employed to account for different real environments. Calculations were performed on poly(dG)-poly(dC), telomeric-DNA, random-ATGC DNA and λ -DNA. The authors find that random and λ -DNA have localisation lengths allowing for electron motion among a few dozen base pairs only. An enhancement of localisation lengths similar to the fishbone model (7) was observed at particular energies for an increasing binary backbone disorder. In Refs. [100,115], the model was used to study differences in different natural and artificial DNA sequences. Specifically, promoter sequences and sequences known to be repetitive from a biological point of view were investigated to see whether there were statistically relevant differences. Using the same sequences as Ref. [89], no support for larger ξ values in regions of coding DNA was found.

5 Conclusions

In this chapter, we have aimed at giving a review of current models used for a simplified, tight-binding-based analysis of charge transport in DNA. While the models can be roughly classified according to their geometrical structure, many of the presently available results appear somewhat disjoint and are nearly as widely spread as in the experimental situation. Let us nevertheless attempt to identify some common themes. The vast majority of studies presented here agrees that the transport properties upon including some degree of energetic disorder — be it strictly random or according to some suitable, naturally occurring sequence — tend towards the insulating side. Nevertheless, the size of the electronic states for finite DNA strands might be larger and even exceed the distance between contacts. In such a situation, the experimental results might find finite currents. This finding seems to be largely independent of the set of on site energies and hopping strengths chosen. Also, most studies agree that there are differences between natural DNA sequences and random DNA with the same ATGC content. However, it is not clear if these differences are due to the special choice of DNA strands and simply become statistically irrelevant when other DNA sequences are considered as well. Thus, a clear correlation between charge transport and a particular DNA sequence or parts thereof is yet to be discovered. We emphasize, however, that if such a correlation were to be found, we would find it useful if it persists across most models reviewed here.

Acknowledgments

It is a pleasure to thank H. Burgert, R. Di Felice, D. Hodgson, R. Gutierrez, D. Porath, R. A. Remer, S. Roche, C. T. Shih, A. Troisi, M. S. Turner and E. B. Starikov for stimulating discussions and collaborations on topics related to this chapter. File hosting has been provided for free by CVSDude.org.

G.C. would like to acknowledge support by the the Volkswagen Foundation under grant No. I/78 340, the DFG priority program “SPP 1243”, the European Union grant DNAnanoDEVICES under contract No. IST-029192-2, the German Israeli Foundation grant No. 190/2006, and the Hans Vielberth Foundation. E.M. has been supported by the Universidad Complutense de Madrid through project PR27/05-14014-BSCH. R.A.R. thankfully acknowledges support by the EPSRC (EP/C007042/1), the Royal Society and the Leverhulme Trust.

References

1. *Modern Methods for Theoretical Physical Chemistry of Biopolymers*, edited by E. B. Starikov, J. P. Lewis, and S. Tanaka (Elsevier, Amsterdam, 2006).
2. D. D. Eley and D. I. Spivey, *Trans. Faraday Soc.* **58**, 411 (1962).
3. S. O. Kelley and J. K. Barton, *Science* **283**, 375 (1999).
4. K. Keren, R. S. Berman, E. Buchstab, U. Sivan, and E. Braun, *Science* **302**, 1380 (2003).
5. M. Mertig, R. Kirsch, W. Pompe, and H. Engelhardt, *Eur. Phys. J. D* **9**, 45 (1999).
6. J. H. Reif, T. H. LaBean, and N. C. Seeman, in *DNA '00: Revised Papers from the 6th International Workshop on DNA-Based Computers* (Springer-Verlag, London, UK, 2001), pp. 173–198.
7. C. J. Murphy, M. A. Arkin, Y. Jenkins, N. D. Ghatlia, S. Bossman, N. J. Turro, and J. K. Barton, *Science* **262**, 1025 (1993).
8. S. Priyadarshy, S. M. Risser, and D. N. Beratan, *J. Phys. Chem.* **100**, 17678 (1996).
9. E. Meggers, M. E. Michel-Beyerle, and B. Giese, *J. Am. Chem. Soc.* **120**, 12950 (1998).
10. C. R. Treadway, M. G. Hill, and J. K. Barton, *Chemical Physics* **281**, 409 (2002).
11. E. Braun, Y. Eichen, U. Sivan, and G. Ben-Yoseph, *Nature* **391**, 775 (1998).
12. A. J. Storm, J. van Noort, S. de Vries, and C. Dekker, *Appl. Phys. Lett.* **79**, 3881 (2001).
13. D. Porath, A. Bezryadin, S. de Vries, and C. Dekker, *Nature* **403**, 635 (2000).
14. H. Cohen, C. Noguez, R. Naaman, and D. Porath, *Proc. Nat. Acad. Sci.* **102**, 11589 (2005).
15. H.-W. Fink and C. Schonenberger, *Nature* **398**, 407 (1999).
16. K.-H. Yoo, D. H. Ha, J.-O. Lee, J. W. Park, J. Kim, J. J. Kim, H.-Y. Lee, T. Kawai, and H. Y. Choi, *Phys. Rev. Lett.* **87**, 198102 (2001).
17. B. Xu, P. Zhang, X. Li, and N. Tao, *Nano Lett.* **4**, 1105 (2004).
18. A. Y. Kasumov, M. Kociak, S. Guéron, B. Reulet, V. T. Volkov, D. V. Klinov, and H. Bouchiat, *Science* **291**, 280 (2001).
19. E. Artacho, M. Machado, D. Sanchez-Portal, P. Ordejon, and J. M. Soler, *Mol. Phys.* **101**, 1587 (2003).
20. A. Calzolari, R. Di Felice, E. Molinari, and A. Garbesi, *Appl. Phys. Lett.* **80**, 3331 (2002).
21. R. Di Felice, A. Calzolari, and H. Zhang, *Nanotechnology* **15**, 1256 (2004).

22. F. L. Gervasio, P. Carolini, and M. Parrinello, *Phys. Rev. Lett.* **89**, 108102 (2002).
23. R. N. Barnett, C. L. Cleveland, A. Joy, U. Landman, and G. B. Schuster, *Science* **294**, 567 (2001).
24. A. Hübsch, R. G. Endres, D. L. Cox, and R. R. P. Singh, *Phys. Rev. Lett.* **94**, 178102 (2005).
25. E. B. Starikov, *Phil. Mag. Lett.* **83**, 699 (2003).
26. E. B. Starikov, *Phil. Mag.* **85**, 3435 (2005).
27. C. Adessi, S. Walch, and M. P. Anantram, *Phys. Rev. B* **67**, 081405(R) (2003).
28. H. Mehrez and M. P. Anantram, *Phys. Rev. B* **71**, 115405 (2005).
29. G. Cuniberti, L. Craco, D. Porath, and C. Dekker, *Phys. Rev. B* **65**, 241314 (2002).
30. J. Jortner, M. Bixon, T. Langenbacher, and M. E. Michel-Beyerle, *Proc. Nat. Acad. Sci.* **95**, 12759 (1998).
31. J. Jortner and M. Bixon, *Chemical Physics* **281**, 393 (2002).
32. S. Roche, D. Bicout, E. Maciá, and E. Kats, *Phys. Rev. Lett.* **91**, 228101 (2003).
33. S. Roche, *Phys. Rev. Lett.* **91**, 108101 (2003).
34. M. Unge and S. Stafstrom, *Nano Lett.* **3**, 1417 (2003).
35. F. Palmero, J. F. R. Archilla, D. Hennig, and F. R. Romero, *New J. Phys.* **6**, 13 (2004).
36. V. M. Apalkov and T. Chakraborty, *Phys. Rev. B* **71**, 033102 (2005).
37. V. M. Apalkov and T. Chakraborty, *Phys. Rev. B* **72**, 161102 (2005).
38. R. Gutierrez, S. Mandal, and G. Cuniberti, *Phys. Rev. B* **71**, 235116 (2005).
39. R. Gutierrez, S. Mandal, and G. Cuniberti, *Nano Lett.* **5**, 1093 (2005), ArXiv: cond-mat/0410660.
40. D. K. Klotsa, R. A. Römer, and M. S. Turner, *Biophys. J.* **89**, 2187 (2005).
41. H. Yamada, *Phys. Lett. A* **332**, 65 (2004), cond-mat/0406040.
42. M. R. D'Orsogna and R. Bruinsma, *Phys. Rev. Lett.* **90**, 078301 (2003).
43. E. Maciá and S. Roche, *Nanotechnology* **17**, 3002 (2006).
44. E. Maciá, *Phys. Rev. B* **74**, 245105 (2006).
45. O. R. Davies and J. E. Inglesfield, *Phys. Rev. B* **69**, 195110 (2004).
46. Y. J. Yan and H. Zhang, *J. Theor. Comput. Chem.* **1**, 225 (2002).
47. K. Iguchi, *Int. J. Mod. Phys. B* **18**, 1845 (2004).
48. A. A. Voityuk, J. Jortner, M. Boxin, and N. Rösch, *J. Chem. Phys.* **114**, 5614 (2001).
49. H. Sugiyama and I. Saito, *J. Am. Chem. Soc.* **118**, 7063 (1996).
50. H. Zhang, X.-Q. Li, P. Han, X. Y. Yu, and Y. Yan, *J. Chem. Phys.* **117**, 4578 (2002).
51. X. Yang, X.-B. Wang, E. R. Vorpagel, and L.-S. Wang, *Proc. Nat. Acad. Sci.* **101**, 17588 (2004).
52. E. Cauet, D. Dehareng, and J. Lievin, *J. Phys. Chem. A* **110**, 9200 (2006).
53. *Computational Statistical Physics: From Billiards to Monte Carlo*, edited by K. H. Hoffmann and M. Schreiber (Springer-Verlag, Berlin, 2002).
54. B. Kramer and A. MacKinnon, *Rep. Prog. Phys.* **56**, 1469 (1993).
55. R. A. Römer and M. Schreiber, in *The Anderson Transition and its Ramifications — Localisation, Quantum Interference, and Interactions*, Vol. 630 of *Lecture Notes in Physics*, edited by T. Brandes and S. Kettmann (Springer, Berlin, 2003), Chap. Numerical investigations of scaling at the Anderson transition, pp. 3–19.

56. P. J. Pablo, F. Moreno-Herrero, J. Colchero, J. Gomez Herrero, P. Hererro, P. Baro, A. M. an Ordejon, J. M. Soler, and E. Artacho, *Phys. Rev. Lett.* **85**, 4992 (2000).
57. B. Alberts, D. Bray, J. Lewis, M. Raff, K. Roberts, and J. Watson, *Molecular Biology of the Cell* (Garland, New York, 1994).
58. A. MacKinnon, *J. Phys.: Condens. Matter* **13**, L1031 (1980).
59. A. MacKinnon, *Z. Phys. B* **59**, 385 (1985).
60. R. A. Römer, C. Villagonzalo, and A. MacKinnon, *J. Phys. Soc. Japan* **72**, 167 (2003), suppl. A.
61. A. Croy, R. A. Römer, and M. Schreiber, in *Parallel Algorithms and Cluster Computing - Implementations, Algorithms, and Applications, Lecture Notes in Computational Science and Engineering*, edited by K. Hoffmann and A. Meyer (Springer, Berlin, 2006), Chap. Localization of electronic states in amorphous materials: recursive Green function method and the metal-insulator transition at $E \neq 0$.
62. J. D'Amato and H. Pastawski, *Phys. Rev. B* **41**, 7411 (1990).
63. J.-L. Pichard and G. Sarma, *J. Phys. C* **14**, L127 (1981).
64. J.-L. Pichard and G. Sarma, *J. Phys. C* **14**, L617 (1981).
65. A. MacKinnon and B. Kramer, *Z. Phys. B* **53**, 1 (1983).
66. A. MacKinnon, *J. Phys.: Condens. Matter* **6**, 2511 (1994).
67. K. Frahm, A. Müller-Groeling, J. L. Pichard, and D. Weinmann, *Europhys. Lett.* **31**, 169 (1995).
68. R. A. Römer and M. Schreiber, *Phys. Rev. Lett.* **78**, 4890 (1997).
69. M. L. Ndawana, R. A. Römer, and M. Schreiber, *Europhys. Lett.* **68**, 678 (2004).
70. M. Büttiker, Y. Imry, and R. Landauer, *Phys. Lett. A* **96**, 365 (1983).
71. M. Büttiker, Y. Imry, R. Landauer, and S. Pinhas, *Phys. Rev. B* **31**, 6207 (1985).
72. P. F. Bagwell and T. P. Orlando, *Phys. Rev. B* **40**, 1456 (1989).
73. E. G. Emberly and G. Kirczenow, *Phys. Rev. B* **58**, 10911 (1998).
74. E. G. Emberly and G. Kirczenow, *J. Phys.: Condens. Matter* **11**, 6911 (1999).
75. T. Kostyrko, *J. Phys.: Condens. Matter* **14**, 4393 (2002).
76. E. Maciá, F. Triozon, and S. Roche, *Phys. Rev. B* **71**, 113106 (2005).
77. Y. Zhu, C. C. Kaun, and H. Guo, *Phys. Rev. B* **69**, 245112 (2004).
78. B. Hartzell, B. Melord, D. Asare, H. Chen, J. J. Heremans, and V. Sughomnian, *Appl. Phys. Lett.* **82**, 4800 (2003).
79. Y. Zhang, R. H. Austin, J. Kraeft, E. C. Cox, and N. P. Ong, *Phys. Rev. Lett.* **89**, 198102 (2002).
80. P. W. Anderson, *Phys. Rev.* **109**, 1492 (1958).
81. *The Anderson Transition and its Ramifications — Localisation, Quantum Interference, and Interactions*, Vol. 630 of *Lecture Notes in Physics*, edited by T. Brandes and S. Kettemann (Springer, Berlin, 2003).
82. X.-Q. Li and Y. Yan, *Appl. Phys. Lett.* **79**, 2190 (2001).
83. S. Datta, *Electronic Transport in Mesoscopic Systems* (Cambridge University Press, Cambridge, 1999).
84. Z. Yu and X. Song, *Phys. Rev. Lett.* **86**, 6018 (2001).
85. W. Zhang and S. E. Ulloa, *Phys. Rev. B* **69**, 153203 (2004).
86. Y. Asai, *J. Phys. Chem. B* **107**, 4647 (2003).
87. E. L. Alburquerque, M. S. Vasconcelos, M. L. Lyra, and F. A. B. F. de Moura, *Phys. Rev. E* **71**, 21910 (2005).

88. C.-T. Shi, *phys. stat. sol. (b)* **243**, 378 (2006).
89. C. T. Shih, *Phys. Rev. E* **74**, 010903 (2006).
90. E. M. Conwell and S. V. Rakhmanova, *Proc. Nat. Acad. Sci.* **97**, 4556 (2000).
91. R. Bruinsma, G. Grüner, M. R. D'Orsogna, and J. Rudnick, *Phys. Rev. Lett.* **85**, 4393 (2000).
92. W. Zhang, A. O. Govorov, and S. E. Ulloa, *Phys. Rev. B* **66**, 060303 (2002).
93. S. Komineas, G. Kalosakas, and A. R. Bishop, *Phys. Rev. E* **65**, 061905 (2002).
94. H. Yamada, E. B. Starikov, D. Hennig, and J. F. R. Archilla, *Eur. Phys. J. E* **17**, 149 (2004), ArXiv: cond-mat/0407148.
95. F. C. Grozema, Y. A. Berlin, and L. D. A. Siebbeles, *J. Am. Chem. Soc.* **122**, 10903 (2000).
96. R. G. Endres, D. L. Cox, R. R. P. Singh, and S. K. Pati, *Phys. Rev. Lett.* **88**, 166601 (2002), ArXiv: cond-mat/0009018.
97. E. I. Kats and V. V. Lebedev, *JETP Lett.* **75**, 37 (2002).
98. V. D. Lakhno, *J. Biol. Phys.* **26**, 133 (2000).
99. N. Rösch and A. A. Voityuk, *Top. curr. chem.* **237**, 37 (2004). See Ref. [116].
100. H. Wang, R. Marsh, J. P. Lewis, and R. A. Römer, in *Modern Methods for Theoretical Physical Chemistry of Biopolymers*, edited by E. B. Starikov, J. P. Lewis, and S. Tanaka (Elsevier, Amsterdam, 2006), Chap. Electronic transport and localization in short and long DNA, pp. 407–428.
101. R. A. Römer and H. Schulz-Baldes, *Europhys. Lett.* **68**, 247 (2004).
102. K. Iguchi, *Int. J. Mod. Phys. B* **11**, 2405 (1997).
103. J. Yi, *Phys. Rev. B* **68**, 193103 (2004).
104. R. A. Caetano and P. A. Schulz, *Phys. Rev. Lett.* **95**, 126601 (2005).
105. A. Sedrakyan and F. Domínguez-Adame, *Phys. Rev. Lett.* **96**, 059703 (2006).
106. R. A. Caetano and P. A. Schulz, *Phys. Rev. Lett.* **96**, 059704 (2006).
107. E. Díaz, A. Sedrakyan, D. Sedrakyan, and F. Domínguez-Adame, *Phys. Rev. B* **75**, 014201 (2007).
108. K. Iguchi, *J. Phys. Soc. Jpn.* **70**, 593 (2001).
109. K. Forinash, A. R. Bishop, and P. S. Lomdahl, *Phys. Rev. B* **43**, 10743 (1991).
110. N. R. Walet and W. J. Zakrzewski, *Nonlinearity* **18**, 2615 (2005), ArXiv: cond-mat/0402059v1.
111. S. S. Wesolowski, M. L. Leininger, P. N. Pentchev, and H. F. Schaefer III, *J. Am. Chem. Soc.* **123**, 4023 (2001).
112. J. Zhong, in *Proceedings of the 2003 Nanotechnology Conference, Computational Publications*, edited by M. Laudon and B. Romamowicz (Nano Science and Technology Institute, Cambridge, 2003), Vol. 2, pp. 105–108, (Molecular and Nano Electronics).
113. D. K. Klotsa, R. A. Römer, and M. S. Turner, In *Proceedings 27th International Conference on the Physics of Semiconductors(Q5 129)*, Flagstaff, Arizona 328 (2004).
114. R. G. Endres, D. L. Cox, and R. P. Singh, *Rev. Mod. Phys.* **76**, 195 (2004).
115. A. Rodriguez, R. A. Römer, and M. S. Turner, *phys. stat. sol. (b)* **243**, 373 (2005).
116. *Long-Range Charge Transfer in DNA I and II*, Vol. 237 of *Topics in Current Chemistry*, edited by G. B. Schuster (Springer, Berlin, 2004), .